Research Article | Vol. 9, No. 6 | 1 Jun 2018 | BIOMEDICAL OPTICS EXPRESS 2604
Biomedical Optics EXPRESS

Rapid, large-scale stimulated Raman histology with strip mosaicing and dual-phase detection

Bohan Zhang,[1] Mengxiong Sun,[2] Yifan Yang,[1] Lingchao Chen,[3] Xiang Zou,[3] Tian Yang,[4] Yingqi Hua,[2] and Minbiao Ji[1]

[1]*State Key Laboratory of Surface Physics and Department of Physics, Collaborative Innovation Center of Genetics and Development, Key Laboratory of Micro and Nano Photonic Structures (Ministry of Education), Fudan University, Shanghai 200433, China*
[2]*Department of Orthopedics, Shanghai General Hospital, Shanghai Jiao Tong University School of Medicine, Shanghai 200080, China*
[3]*Department of Neurosurgery, Huashan Hospital, Fudan University, Shanghai 200040, China*
[4]*Department of Hepatobiliary Surgery, the Eastern Hepatobiliary Surgery Hospital, the Second Military Medical University, Shanghai 200433, China*
**minbiaoj@fudan.edu.cn*

Abstract: Two-color stimulated Raman scattering (SRS) microscopy with label-free mapping of lipid/protein distributions has shown promise in virtual histology. Despite previous demonstrations of SRS in tumor delineation and diagnosis, the speed and efficiency of the current technique requires further improvements for practical use. Here, we integrate parallel dual-phase SRS detection with strip mosaicing, which reduces the imaging time of a whole mouse brain section from 70 to 8 minutes. We further verified our method in imaging fresh human surgical tissues, showing its great potential for rapid SRS histology, especially for large scale, large quantity imaging tasks.

OCIS codes: (220.4830) Systems design; (170.0110) Imaging systems; (290.5910) Scattering, stimulated Raman; (170.5660) Raman spectroscopy.

References and links

1. C. W. Freudiger, W. Min, B. G. Saar, S. Lu, G. R. Holtom, C. He, J. C. Tsai, J. X. Kang, and X. S. Xie, "Label-free biomedical imaging with high sensitivity by stimulated Raman scattering microscopy," Science **322**(5909), 1857–1861 (2008).
2. B. G. Saar, C. W. Freudiger, J. Reichman, C. M. Stanley, G. R. Holtom, and X. S. Xie, "Video-rate molecular imaging in vivo with stimulated Raman scattering," Science **330**(6009), 1368–1370 (2010).
3. E. Ploetz, S. Laimgruber, S. Berner, W. Zinth, and P. Gilch, "Femtosecond stimulated Raman microscopy," Appl. Phys. B **87**(3), 389–393 (2007).
4. A. Zumbusch, G. R. Holtom, and X. S. Xie, "Three-dimensional vibrational imaging by coherent anti-Stokes Raman scattering," Phys. Rev. Lett. **82**(20), 4142–4145 (1999).
5. J. X. Cheng and X. S. Xie, "Vibrational spectroscopic imaging of living systems: An emerging platform for biology and medicine," Science **350**(6264), aaa8870 (2015).
6. C. W. Freudiger, R. Pfannl, D. A. Orringer, B. G. Saar, M. Ji, Q. Zeng, L. Ottoboni, Y. Wei, C. Waeber, J. R. Sims, P. L. De Jager, O. Sagher, M. A. Philbert, X. Xu, S. Kesari, X. S. Xie, and G. S. Young, "Multicolored stain-free histopathology with coherent Raman imaging," Lab. Invest. **92**(10), 1492–1502 (2012).
7. D. Fu, J. Zhou, W. S. Zhu, P. W. Manley, Y. K. Wang, T. Hood, A. Wylie, and X. S. Xie, "Imaging the intracellular distribution of tyrosine kinase inhibitors in living cells with quantitative hyperspectral stimulated Raman scattering," Nat. Chem. **6**(7), 614–622 (2014).
8. M. C. Wang, W. Min, C. W. Freudiger, G. Ruvkun, and X. S. Xie, "RNAi screening for fat regulatory genes with SRS microscopy," Nat. Methods **8**(2), 135–138 (2011).
9. D. Fu, F. K. Lu, X. Zhang, C. Freudiger, D. R. Pernik, G. Holtom, and X. S. Xie, "Quantitative chemical imaging with multiplex stimulated Raman scattering microscopy," J. Am. Chem. Soc. **134**(8), 3623–3626 (2012).
10. M. Ji, D. A. Orringer, C. W. Freudiger, S. Ramkissoon, X. Liu, D. Lau, A. J. Golby, I. Norton, M. Hayashi, N. Y. Agar, G. S. Young, C. Spino, S. Santagata, S. Camelo-Piragua, K. L. Ligon, O. Sagher, and X. S. Xie, "Rapid, label-free detection of brain tumors with stimulated Raman scattering microscopy," Sci. Transl. Med. **5**(201), 201ra119 (2013).
11. M. Ji, S. Lewis, S. Camelo-Piragua, S. H. Ramkissoon, M. Snuderl, S. Venneti, A. Fisher-Hubbard, M. Garrard, D. Fu, A. C. Wang, J. A. Heth, C. O. Maher, N. Sanai, T. D. Johnson, C. W. Freudiger, O. Sagher, X. S. Xie, and

#325237 https://doi.org/10.1364/BOE.9.002604
Journal © 2018 Received 14 Mar 2018; revised 7 May 2018; accepted 8 May 2018; published 10 May 2018

Biomedical Optics EXPRESS

D. A. Orringer, "Detection of human brain tumor infiltration with quantitative stimulated Raman scattering microscopy," Sci. Transl. Med. **7**(309), 309ra163 (2015).
12. Y. Yang, L. Chen, and M. Ji, "Stimulated Raman scattering microscopy for rapid brain tumor histology," J. Innov. Opt. Health Sci. **11**(2), 1730010–1730021 (2017).
13. F. K. Lu, D. Calligaris, O. I. Olubiyi, I. Norton, W. Yang, S. Santagata, X. S. Xie, A. J. Golby, and N. Y. Agar, "Label-Free Neurosurgical Pathology with Stimulated Raman Imaging," Cancer Res. **76**(12), 3451–3462 (2016).
14. F. K. Lu, S. Basu, V. Igras, M. P. Hoang, M. Ji, D. Fu, G. R. Holtom, V. A. Neel, C. W. Freudiger, D. E. Fisher, and X. S. Xie, "Label-free DNA imaging in vivo with stimulated Raman scattering microscopy," Proc. Natl. Acad. Sci. U.S.A. **112**(37), 11624–11629 (2015).
15. D. A. Orringer, B. Pandian, Y. S. Niknafs, T. C. Hollon, J. Boyle, S. Lewis, M. Garrard, S. L. Hervey-Jumper, H. J. L. Garton, C. O. Maher, J. A. Heth, O. Sagher, D. A. Wilkinson, M. Snuderl, S. Venneti, S. H. Ramkissoon, K. A. McFadden, A. Fisher-Hubbard, A. P. Lieberman, T. D. Johnson, X. S. Xie, J. K. Trautman, C. W. Freudiger, and S. Camelo-Piragua, "Rapid intraoperative histology of unprocessed surgical specimens via fibre-laser-based stimulated Raman scattering microscopy," Nat Biomed Eng **1**(2), 0027 (2017).
16. C. W. Freudiger, W. Yang, G. R. Holtom, N. Peyghambarian, X. S. Xie, and K. Q. Kieu, "Stimulated Raman Scattering Microscopy with a Robust Fibre Laser Source," Nat. Photonics **8**(2), 153–159 (2014).
17. C.-S. Liao, P. Wang, C. Y. Huang, P. Lin, G. Eakins, R. T. Bentley, R. Liang, and J.-X. Cheng, "In vivo and in situ spectroscopic imaging by a handheld stimulated Raman scattering microscope," ACS Photonics **5**(3), 947–954 (2017).
18. R. He, Y. Xu, L. Zhang, S. Ma, X. Wang, D. Ye, and M. Ji, "Dual-phase stimulated Raman scattering microscopy for real-time two-color imaging," Optica **4**(1), 44–47 (2017).
19. F.-K. Lu, M. Ji, D. Fu, X. Ni, C. W. Freudiger, G. Holtom, and X. S. Xie, "Multicolor stimulated Raman scattering (SRS) microscopy," Mol. Phys. **110**(15-16), 1927–1932 (2012).
20. S. Abeytunge, Y. Li, B. Larson, R. Toledo-Crow, and M. Rajadhyaksha, "Rapid confocal imaging of large areas of excised tissue with strip mosaicing," J. Biomed. Opt. **16**(5), 050504 (2011).
21. R. He, Z. Liu, Y. Xu, W. Huang, H. Ma, and M. Ji, "Stimulated Raman scattering microscopy and spectroscopy with a rapid scanning optical delay line," Opt. Lett. **42**(4), 659–662 (2017).
22. D. Fu, G. Holtom, C. Freudiger, X. Zhang, and X. S. Xie, "Hyperspectral imaging with stimulated Raman scattering by chirped femtosecond lasers," J. Phys. Chem. B **117**(16), 4634–4640 (2013).
23. L. Zhang, S. Shen, Z. Liu, and M. Ji, "Label-Free, Quantitative Imaging of MoS2-Nanosheets in Live Cells with Simultaneous Stimulated Raman Scattering and Transient Absorption Microscopy," Advanced Biosystems **1**(4), 1700013–1700020 (2017).
24. Y. Xu, Q. Liu, R. He, X. Miao, and M. Ji, "Imaging Laser-Triggered Drug Release from Gold Nanocages with Transient Absorption Lifetime Microscopy," ACS Appl. Mater. Interfaces **9**(23), 19653–19661 (2017).
25. D. N. Louis, A. Perry, G. Reifenberger, A. von Deimling, D. Figarella-Branger, W. K. Cavenee, H. Ohgaki, O. D. Wiestler, P. Kleihues, and D. W. Ellison, "The 2016 World Health Organization classification of tumors of the central nervous system:A summary," Acta Neuropathol. **131**(6), 803–820 (2016).
26. P. J. Campagnola, A. C. Millard, M. Terasaki, P. E. Hoppe, C. J. Malone, and W. A. Mohler, "Three-dimensional high-resolution second-harmonic generation imaging of endogenous structural proteins in biological tissues," Biophys. J. **82**(1 Pt 1), 493–508 (2002).
27. P. J. Campagnola and L. M. Loew, "Second-harmonic imaging microscopy for visualizing biomolecular arrays in cells, tissues and organisms," Nat. Biotechnol. **21**(11), 1356–1360 (2003).
28. X. Han, R. M. Burke, M. L. Zettel, P. Tang, and E. B. Brown, "Second harmonic properties of tumor collagen: determining the structural relationship between reactive stroma and healthy stroma," Opt. Express **16**(3), 1846–1859 (2008).
29. C. S. Liao, M. N. Slipchenko, P. Wang, J. Li, S. Y. Lee, R. A. Oglesbee, and J. X. Cheng, "Microsecond Scale Vibrational Spectroscopic Imaging by Multiplex Stimulated Raman Scattering Microscopy," Light Sci. Appl. **4**(3), e265 (2015).
30. A. Li, H. Gong, B. Zhang, Q. Wang, C. Yan, J. Wu, Q. Liu, S. Zeng, and Q. Luo, "Micro-Optical Sectioning Tomography to Obtain a High-Resolution Atlas of the Mouse Brain," Science **330**(6009), 1404–1408 (2010).

1. Introduction

Imaging techniques capable of providing rapid and sufficient histological information are highly desired in time-sensitive pathologies, such as intraoperative diagnosis. Stimulated Raman scattering (SRS) microscopy has experienced rapid developments in the past decade [1–5], and shown success in various biomedical researches, including label-free tissue imaging [6], drug delivery [7], lipid metabolism [8], and quantitative chemical analysis [9]. Particularly, SRS has demonstrated great potential for rapid virtual histology without exogenous staining, in both live animals and human brain surgical tissues [10–13]. These advances strongly rely on the unique chemical resolution of SRS microscopy, because of the inherent Raman spectroscopy that differentiates various biomolecules, including lipids, proteins and DNA [14]. In addition, bedside SRS microscope based on fiber lasers has been

Biomedical Optics EXPRESS

manufactured and applied in the operating room [15, 16], and SRS handheld device is making its way to miniaturization [17]. Although the imaging speed of SRS is orders of magnitude faster than spontaneous Raman microscopy, the efficiency of current SRS microscope in imaging large-scale tissues remains to be optimized, which is critical for practical applications for rapid, label-free histology.

Two major aspects that limit the speed of SRS histology include: 1) the imaging rate of multi-color SRS, and 2) the efficiency of image mosaicing. It has been the long-term pursuits to achieve both higher imaging rate and richer spectroscopic information in the development of SRS microscopy. However, we still have to balance between the number of spectral channels and imaging speed for different applications. Previous studies have shown that lipid/protein based two-color SRS could provide adequate histological contrast to classify different types and grades of brain tumors, similar to the results of H&E (also a two-component modality) [10, 11]. Yet compared with H&E, SRS microscopy does not suffer from the slow tissue preparation process in H&E, such as biopsy, fixation, sectioning and labeling, thus may be potentially used in fast intraoperative diagnosis. We have previously developed a dual-phase lock-in detection method to achieve real-time two-color SRS imaging, which reaches the highest imaging speed as single color SRS [18]. Such a parallel detection method could in principle maximize the imaging rate of SRS histology, while immune to the effect of light scattering through thick fresh tissues as in the grating based detection techniques [19].

In order to image large sized tissues with high spatial resolution, it is usually required to stitch numerous fields of view (FOV) taken sequentially to cover the large areas of interests. The conventional mosaicing method known as “tiling” has the major disadvantage of wasting large amount of time between adjacent FOV for redundant system initialization, data storage and unnecessary pausing [10]. Alternatively, “strip mosaicing” method has been shown to provide equivalent confocal imaging results as in tiling, where the focused laser beam works in the line scan mode and the sample translates at a constant speed in perpendicular to the laser line [20]. Strip mosaicing has obvious speed improvements in imaging large tissues. However, multicolor SRS with sequential spectral imaging is incompatible with strip mosaicing, primarily because of the slight mismatch between replicas of the same strip taken sequentially at different Raman frequencies, generating unwanted features similar to “motion artefacts”. Tiling with sequential frequency tuning further increases the imaging time, which is proportional to the number of frequency channels.

In this work, we have combined dual-phase SRS detection technique with strip mosaicing to maximize the speed of SRS histology. We showed that almost 10 times reduction of the total imaging time of a whole mouse brain coronal section could be achieved, compared with sequential two-color tiling method in commercial Olympus Flouview software. With the dual-phase strip mosaicing technique, imaging a 12 × 7 mm^2 mouse brain section could be completed within 8 minutes. We further demonstrated the feasibility of our method in imaging fresh human surgical specimens with two-color SRS, as well as multi-modality capability with the addition of second harmonic generation (SHG) channel. Our method provides an efficient means to image large area tissues with multi-chemical contrast, which is vitally important in both rapid histology and bulk data accumulation for statistical analysis and machine learning.

2. Materials and methods

2.1 Experimental setup

The experimental design based on the dual-phase SRS microscope is illustrated in Fig. 1. The basic concept and technical details of dual-phase SRS have been reported previously [18]. Briefly, we used pulsed femtosecond laser beams from a commercial optical parametric oscillator (OPO) laser (Insight DS+, Newport, CA) as the light source. We set the fundamental 1040 nm laser as the Stokes beam (~150fs), and the tunable OPO output (690-

Biomedical Optics EXPRESS

1300 nm, ~120fs) as the pump beam. Spectral focusing technique was applied to obtain sufficient spectral resolution [21, 22]. The femtosecond pulses were chirped through high dispersive glass rods (SF57) to several picoseconds, and the target Raman frequency could be tuned by adjusting the time delay τ between pump and Stokes pulses (Fig. 1(a) and (b)). The key idea of dual-phase SRS is to split one of the beams (Stokes beam in our case) into two, set each of them to probe the target Raman frequency, and modulate them with 90° phase difference (Fig. 1(b)). Therefore, SRS signals at Ω_1 and Ω_2 were generated as the in-phase and in-quadrature components. A single photodiode (PD) was used to detect the sum of the two signals, and a phase sensitive lock-in amplifier (HF2LI, Zurich Instrument) was applied to simultaneously demodulate the two orthogonal components through the X and Y output channels, realizing parallel two-color SRS detection. In our setup, we used a single electro-optical modulator (EOM) combined with proper pulse-train control to achieve both the Raman frequency selection and quadrature phase setting. The amplitude of the 1040 nm laser was modulated at 1/4 of the laser repetition rate (f_0 = 80 MHz) with a frequency divider to lock the modulation phase. The two delay lines (DL1 and DL2) were used to fully control the temporal profiles of the pump and two Stokes beams. One pulse interval was added in DL2 to effectively generate quadrature phase shift between the two Stokes beams without changing the SRS intensity. Time delay τ_1 and τ_2 were precisely set to probe the two high-frequency Raman modes at Ω_1 (2845 cm^{-1}) and Ω_2 (2930 cm^{-1}), so that lipid/protein contents could be simultaneously image with minimum crosstalk or interference after proper setting of the reference phase of the lock-in amplifier [18]. All imaging tasks were performed with Olympus FV1200 microscope. Such a dual-phase method not only works for spectral-focusing based SRS microscopy, but also suited for general pump-probe based microscopies [23, 24].

Biomedical Optics EXPRESS

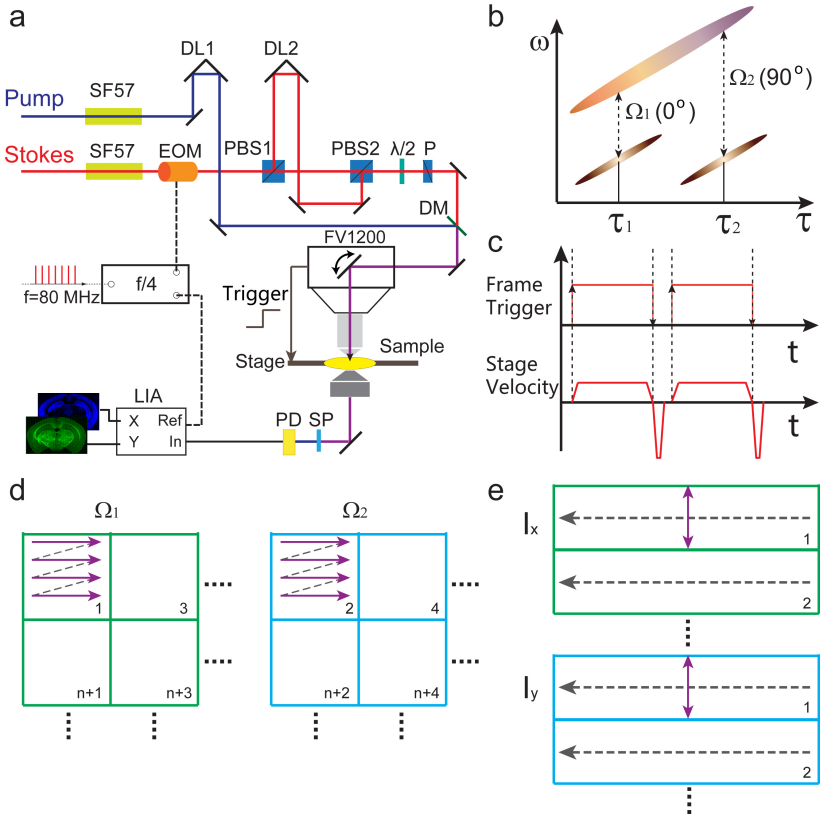

Fig. 1. (a) Optical layout of the experiment setup. (b) Pulse profiles of the pump and two Stokes beams in dual-phase SRS. (c) Frame trigger and sample stage velocity. (d) Illustration of sequential tiling for two Raman frequencies. (e) Illustration of parallel strip mosaicing. SF57: dispersive glass rods; EOM: electro-optical modulator; PBS: polarizing beam splitter; DL: delay line; λ/2:half wave plate; P:polarizer; DM: dichroic mirror; SP: short pass filter; PD: photodiode; LIA: lock-in amplifier.

We integrated the dual-phase technique with strip mosaicing scheme to enable rapid SRS histology. Similar to the technique used in confocal imaging [20], our system combined optical and mechanical scanning to image across large sample areas. As illustrated in Fig. 1(a), the laser beam was continuously scanning in one dimension, while the sample stage was translated in the perpendicular direction at a constant speed to generate image strips. Olympus Fluoview software was set at the "Linescan" mode to scan the laser beam and acquire image data. We built an additional master program with Labview (National Instruments) to synchronize the sample stage (Prior Scientific, ProScan III) with Fluoview software. The stage started to move with the rising edge of the frame TTL signal of FV1200 when each "Linescan" task was initiated. And multiple tasks were pre-programed in Fluoview based on the size of the sample, so that they could be stitched to cover the whole sample. We only collected data in one direction, thus the stage velocity in the "backfly" direction was set to be much faster than the imaging direction (Fig. 1(c)). The imaging time of each strip was calculated based on the length of the strip and the stage velocity, with the inclusion of additional time costs at the acceleration and deceleration period. The stage velocity could be calculated as:

$$V = \frac{W}{T_f} = \frac{W}{2N^2 t_p}. \quad (1)$$

Biomedical Optics EXPRESS

Where W is the length of the scanning laser line (strip width), T_f is the frame imaging time, N is the number of pixels in each line, and t_p is the pixel dwell time. In this setting, the sampling density in X and Y directions are identical, equivalent to the stitching of normal square tiles. And the number of lines in each strip could be estimated as: LN/W, where L is the strip length. In our experiments, W = 509 μm for 25x objective, W = 212 μm for 60x objective, t_p = 2 μs and N = 512.

The comparison between the sequential tiling and parallel strip mosaicing of two-color SRS is schematically illustrated in Figs. 1(d) and (e). In the tiling mode, each tile of the tissue needs to be imaged twice at the two Raman frequencies before moving to the next, and usually several seconds (~3 s) interval exists between adjacent images. By contrast, parallel strip mosaicing avoids the redundant time intervals as wells as the repeated imaging for the two Raman frequencies, hence is as efficient as single color strip mosaicing. Moreover, additional parallel imaging channels could be naturally included in the process to realize multi-modal imaging, such as SHG and two-photon excited fluorescence (TPEF) with photomultiplier tubes (PMT). After completing the data acquisition, the image strips were loaded into our Matlab program for stitching. Note that strip mosaicing reduces one of the stitching dimensions, which helps improving the final image quality with less stitching artefacts. The stitched images at Ω_1 and Ω_2 were then decomposed into the distributions of lipids and proteins following the simple linear algebra, and false colored to form the final two-color images [10].

2.2 Sample preparation

Mice were bred under standard husbandry conditions, and all experiments were performed in accordance with the Animal Care and Use Committee at Fudan University. Frozen and fixed sections were utilized in the mouse brain imaging. Mouse was perfused with PBS and 4% paraformaldehyde in phosphate buffered saline. Then the brains were fixed in 4% PFA overnight at 4 °C, and transferred sequentially to 15% and 30% sucrose after brain sunk to the bottom. Brains were embedded and frozen in O.C.T. compound (Tissue-Tek) and 40 μm serial sections were coronally prepared by frozen microtome (Leica, CM1950) and packaged between a glass slide and coverslip when ready for imaging.

Fresh human tissues were collected from patients, and approved by the Ethics Committee of our collaborating hospitals with informed consent from patients (Huashan Hospital: KY2014-240; Shanghai General Hospital: 2018KY144). Chondrosarcoma and liver samples were obtained from Shanghai General Hospital, meningioma samples were obtained from HuaShan Hospital. All fresh tissues were sandwiched between two coverglasses with a perforated slide to flatten the tissues, and imaged without any further treatment. To keep the tissues fresh, they were delivered with ice bags within 3 hours after resection.

3. Results and discussion

3.1 Imaging of the mouse brain section

We first tested our method by imaging mouse brain coronal sections. We utilized a 25x objective (Olympus, UPLSAPO 25XWMP2) to image the tissues in transmission mode with both sequential tilting and parallel strip mosaicing methods. Figure 2 shows the results of a 12×7 mm^2 mouse brain section, with green representing lipids and blue representing proteins distribution. The total imaging time with the tiling method was about 70 minutes, containing 26×16 tiles for each Raman frequency. Whereas in the dual-phase strip mosaicing mode, the total imaging time of the same tissue was reduced to ~8 minutes. It could be seen that the image qualities of both methods are very comparable, revealing almost identical histo-architectures, including white matter, hippocampus (Figs. 2(c) and (e)), and gray matter (Figs. 2(d) and (f)). As proven in the previous studies, histological features based on the axonal and cellular densities and morphologies could provide key diagnostic information for brain

Biomedical Optics EXPRESS

tumors [10, 11]. Hence, our method has the potential to improve the working efficiency of SRS microscopy in the application of neuropathology.

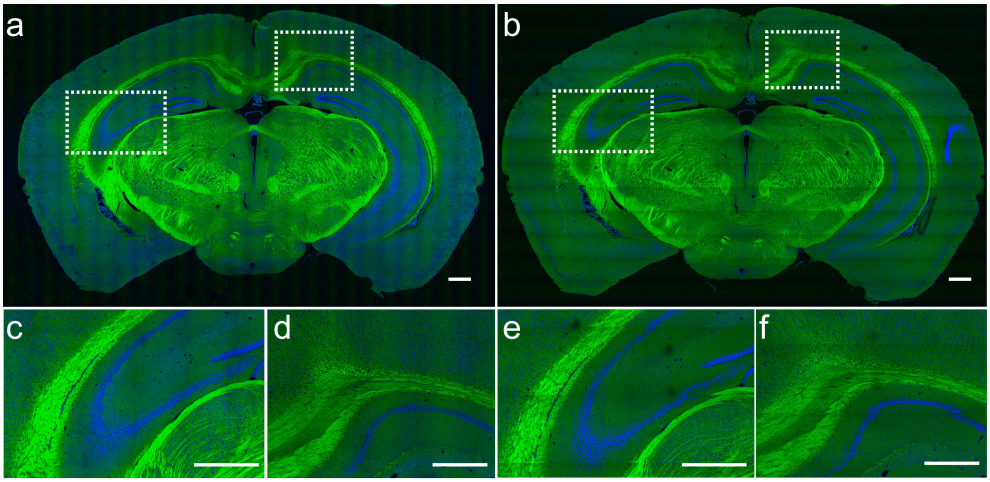

Fig. 2. Two-color SRS images of a mouse brain coronal section imaged with tiling (a) and strip mosaicing (b). Zoomed-in regions of hippocampus and white matter (c, e), and cortext (e, f). Lipids are false colored in green and proteins in blue. Scale bar: 500 μm.

3.2 Imaging fresh human surgical specimens

We next evaluated our method in imaging various types of fresh human tissues excised from the operating room. We chose 60X objective (Olympus, UPLSAPO 60XWIR) to obtain higher spatial resolution, in which case the imaging tasks became heavier and increasing the imaging speed and efficiency became critical. Fresh human chondrosarcoma and liver tissues were imaged and shown in Fig. 3. The total imaging time of these tissues was less than 5 minutes each. In the liver tissue resected from the tumor margin (Figs. 3(a)-(c)), typical features of normal hepatocytes were clearly seen, indicating the possible complete tumor resection. Whereas in chondrosarcoma (Figs. 3(d)-(f)), cell nuclear morphologies could be visualized under different magnifications. Obtaining rapid histology of these tissues is extremely helpful for surgeons to define the surgical margins and make critical decisions with improved efficiency. Further work are ongoing with the aim to create statistical results regarding the efficacy of two-color SRS in diagnosing these types of tumor in human specimens.

Biomedical Optics EXPRESS

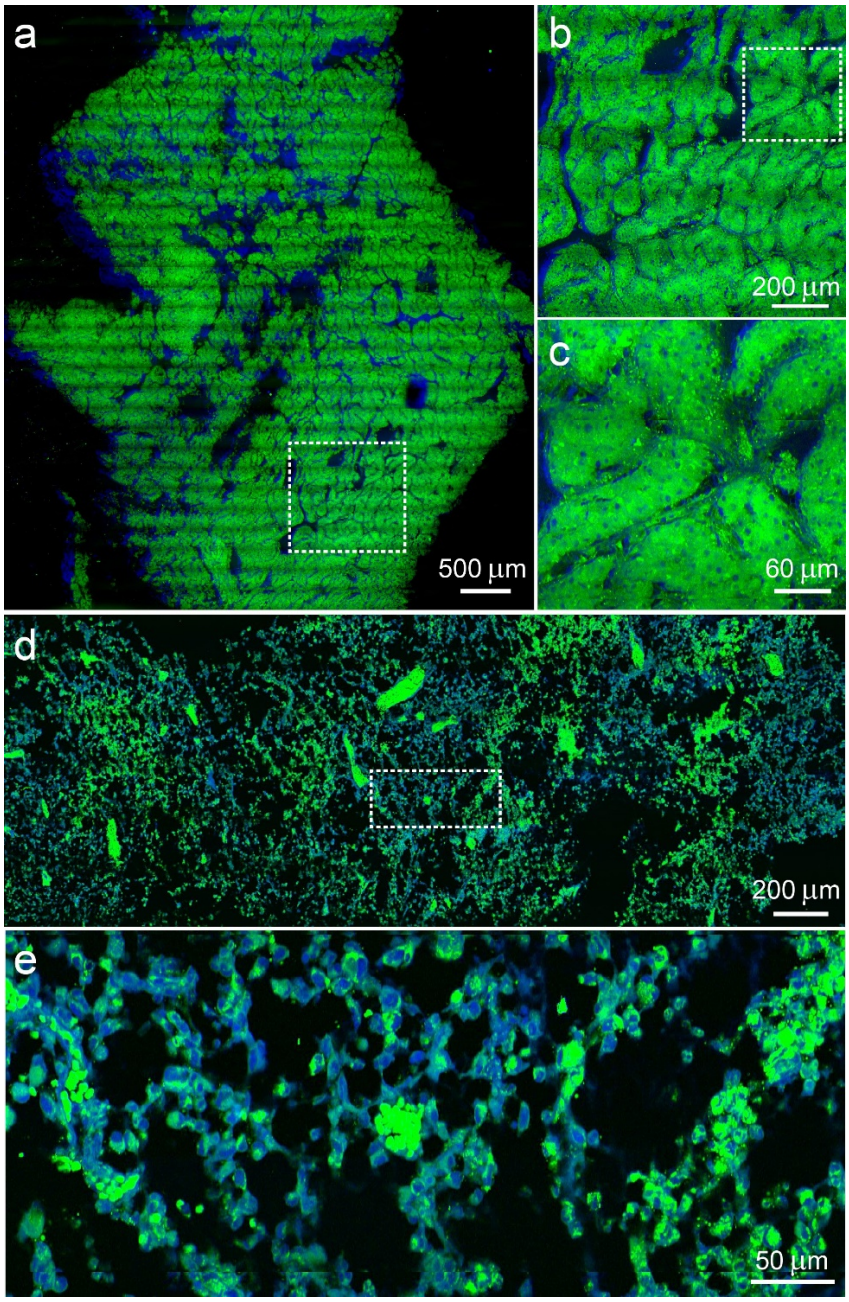

Fig. 3. (a-c) Composite SRS images of human liver tissue taken with SRS strip mosaicing at different scales. (d, e) Human chondrosarcoma tissue imaged with SRS strip mosaicing. Dashed rectangles indicate the zoomed-in areas. Green: lipids; blue: proteins.

3.3 Multi-modal imaging

We further verified that multi-modal imaging could be realized in strip mosaicing method. Figure 4 shows the results of human meningioma, which is a disease with many subtypes [25], thus imaging modalities capable of detecting more chemical compositions will be better suited for the diagnosis. Aside from normal two-color SRS with lipid/protein contrast, SHG can be detected with a narrow band-pass filter and a PMT detector. Many biological

Biomedical Optics EXPRESS

structures have noncentrosymmetric molecular arrangements and therefore can produce large SHG signals given the proper laser excitation field. These structures include collagen, myofilaments, biological membranes and quasi-crystalline tubulin assemblies such as mitotic spindles [26, 27]. In our case, collagen fibers were detected in the SHG channel (Fig. 4(a) and (c)). SHG imaging of collagen fibrils could provide insights into the metastatic pattern of malignant cells [28], and the combination of cellular morphology and collagen fibers may provide important histological inputs for the diagnosis of such a diverse disease. In addition, more imaging channels could also be included (such as TPEF) to image other important biomolecules that generate two-photon autofluoresence, such as elastin and NADH.

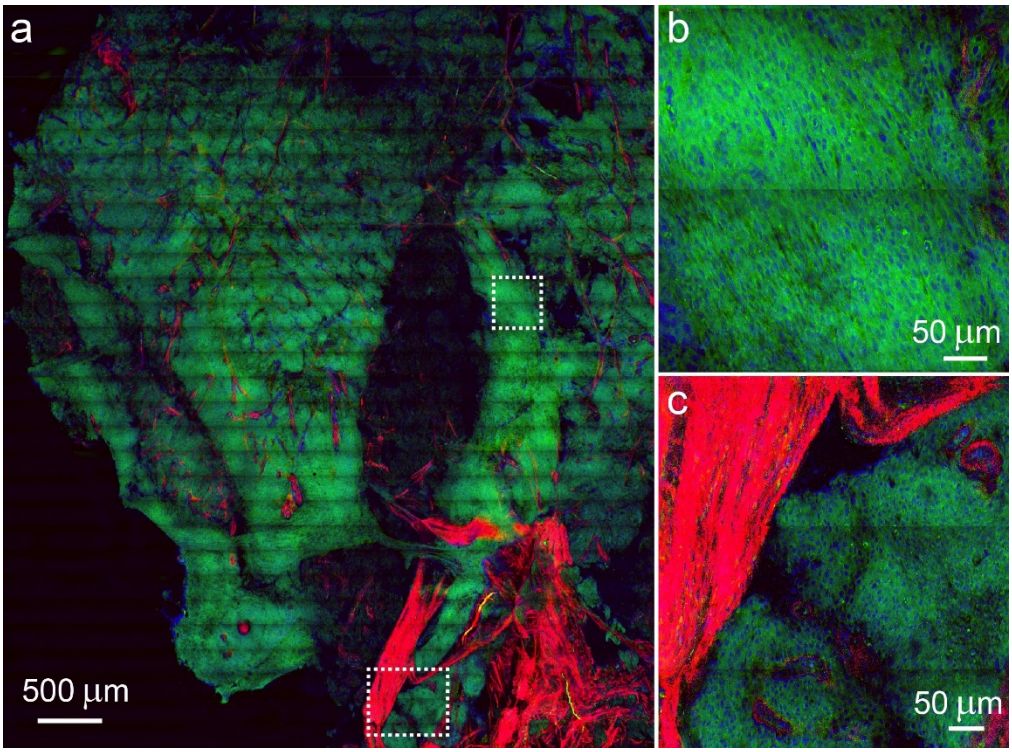

Fig. 4. Multi-modal imaging of a large-area human meningioma tissue with SRS and SHG. (a) Large-scale image of the tissue imaged with strip mosaicing, and zoomed-in regions of the meningioma cells (b) and the boundary with collagen proliferation. Green: lipids; blue: proteins; red: collagen.

4. Discussion

The design of our dual-phase SRS microscopy is not the only way of performing parallel multi-color SRS. In fact, a few other means of multiplex SRS techniques have been developed, including excitation multiplexing and detection multiplexing [9, 19, 29]. In principle, all these parallel detection methods are compatible with strip mosaicing. In reality, the factors including complexity, stability and laser powers need to be considered for practical use. For ordinary two-color SRS histology, our dual-phase method may hold the best opportunity for bedside rapid imaging.

The mosaicing efficiency may be further improved by making full use of bi-directional scanning, which means continuous data collection during bi-directional laser scanning, as well as bi-directional sample movements. To fulfil such a goal, we will need to write our own data acquisition program to optimize image reconstruction with the bi-directional mode, and will be done in the future. With this implementation, the current mosaicing speed is expected

Biomedical Optics EXPRESS

to improve by more than 2 times, and may become the ultimate speed for mosaic imaging with laser scanning microscopes.

The strip mosaicing concept could also be applied in 3D whole mouse brain imaging, where the brain tissues are continuously sliced into thin strips and imaged at the same time [30]. In principle, two-color SRS imaging of a whole mouse brain could be conducted by scanning the laser beams in one dimension while the tissue is translated in perpendicular and sliced layer by layer, over the whole tissue volume. Although technically feasible, it is challenging to figure out the neural connections in SRS images with dense axons.

5. Conclusions

In summary, we have demonstrated that strip mosaicing could be efficiently adapted with dual-phase SRS microscopy, providing a rapid means of acquiring label-free histology on large-scale tissues. By parallel detection and strip mosaicing, our method greatly reduces the total imaging time without sacrificing image quality. We believe our method provides the opportunity for improving the efficiency of intraoperative diagnosis, as well as large data collection for profound analysis, such as machine learning.

Funding

National Key R&D Program of China (2016YFC0102100, 2016YFA0203900); National Natural Science Foundation of China (81671725); Shanghai Rising Star Program (15QA1400500); Shanghai Action Plan for Scientific and Technological Innovation Program (16441909200); and Shanghai Municipal Science and Technology Major Project (2017SHZDZX01).

Acknowledgements

We would like to thank Drs. Yongkui Xu and Ruoyu He for help with the optical setup.

Disclosures

The authors declare that there are no conflicts of interest related to this article.